

# EPR Dosimetry of Cortical Bone and Tooth Enamel Irradiated with X and Gamma Rays: Study of Energy Dependence

D. A. Schauer,<sup>\*1</sup> M. F. Desrosiers,<sup>†</sup> F. G. Le,<sup>†</sup> S. M. Seltzer<sup>†</sup> and J. M. Links<sup>‡</sup>

<sup>\*</sup>Division of Radiation Health Sciences and <sup>†</sup>Divisions of Nuclear Medicine and Radiation Health Sciences, The Johns Hopkins University, School of Hygiene and Public Health, 615 N. Wolfe Street, Baltimore, Maryland 21205; and <sup>‡</sup>Ionizing Radiation Division, Physics Laboratory, National Institute of Standards and Technology, Technology Administration, U.S. Department of Commerce, Gaithersburg, Maryland 20899

Schauer, D. A., Desrosiers, M. F., Le, F. G., Seltzer, S. M. and Links, J. M. EPR Dosimetry of Cortical Bone and Tooth Enamel Irradiated with X and Gamma Rays: Study of Energy Dependence. *Radiat. Res.* 138, 1-8 (1994).

Previous investigators have reported that the radiation-induced EPR signal intensity in compact or cortical bone increases up to a factor of two with decreasing photon energy for a given absorbed dose. If the EPR signal intensity was dependent on energy, it could limit the application of EPR spectrometry and the additive reirradiation method to obtain dose estimates. We have recently shown that errors in the assumptions governing conversion of measured exposure to absorbed dose can lead to similar "apparent" energy-dependence results. We hypothesized that these previous results were due to errors in the estimated dose in bone, rather than the effects of energy dependence *per se*. To test this hypothesis we studied human adult cortical bone from male and female donors ranging in age from 23 to 95 years, and bovine tooth enamel, using 34 and 138 keV average energy X-ray beams and <sup>137</sup>Cs (662 keV) and <sup>60</sup>Co (1250 keV)  $\gamma$  rays. In a femur from a 47-year-old male (subject 1), there was a difference of borderline significance at the  $\alpha = 0.05$  level in the mean radiation-induced hydroxyapatite signal intensities as a function of photon energy. No other statistically significant differences in EPR signal intensity as a function of photon energy were observed in this subject, or in the tibia from a 23-year-old male (subject 2) and the femur from a 75-year-old female (subject 3). However, there was a trend toward a decrease (12-15%) in signal intensity at the lowest energy compared with the highest energy in subjects 1 and 3. Further analysis of the data from subject 1 revealed that this trend, which is in the opposite direction of previous reports but is consistent with theory, is statistically significant. There were no effects of energy dependence in the tooth samples.

<sup>1</sup>Guest Researcher, National Institute of Standards and Technology, Technology Administration, Department of Commerce.

## INTRODUCTION

The electron paramagnetic resonance (EPR) signal that is used as a measurement of absorbed dose in bone is attributed to a paramagnetic center in the crystalline matrix (hydroxyapatite). This signal is anisotropic with components perpendicular ( $g_{\perp}$ ) and parallel ( $g_{\parallel}$ ) to the external magnetic field. Variation in the intensity of the  $g_{\perp}$  component, for a given absorbed dose, as a function of photon energy has been reported previously (1, 2). The earlier work of Stachowicz *et al.* (1) compared <sup>60</sup>Co  $\gamma$  rays with 250 kVp (0.4 Sn + 0.2 Cu + 1.0 Al) X rays, and they reported that the EPR signal intensity from the lower-energy radiation was approximately a factor of two higher than the value for <sup>60</sup>Co. The authors attributed this observation to differences in initial stopping powers. Copeland *et al.* (2) studied ovine cortical bone and reported that an increased signal intensity is observed at lower photon energies (160 kVp, HVL = 0.5 mm Cu) when compared to <sup>60</sup>Co, but of a much lower magnitude than Stachowicz *et al.* (1) observed.

Pass and Aldrich (3) showed that the EPR signal intensity per unit dose in tooth enamel is the same for 80 kVp X rays and <sup>60</sup>Co  $\gamma$  rays. Recently, Serezhnikov *et al.* (4) reported a 2.4-fold increase in regression coefficients for the low-energy X rays (120 keV effective energy) compared to the <sup>60</sup>Co  $\gamma$  rays. They concluded that this was in reasonable agreement with the energy dependence observed by Iwasaki *et al.* (5), but they did not address the apparent conflict of these data with the work of Pass and Aldrich (3).

In EPR-based bone (or tooth enamel) dosimetry, samples of bone are irradiated with known doses, and the EPR signal intensity is quantified. In practice, the delivered dose is determined from a direct measurement of exposure, which is converted to dose through the use of an  $f$  factor. There are three potential sources of error with this approach. First, we have shown that the choice of bone composition has a significant effect on the computed  $f$  factor, and thus on the estimate of delivered dose (6); this effect is most marked at low energies. Second, we have shown that the use of an equivalent photon

TABLE I  
X- and Gamma-Ray Sources (12) and Dosimetry Information

Photon beam	Filtration	HVL (mm Cu)	Average energy (keV)	Exposure rate [C (kg s) <sup>-1</sup> ]	$f_{\text{bone}}$ [mGy (C kg) <sup>-1</sup> ]	Absorbed dose rate <sup>a</sup> (mGy s <sup>-1</sup> )	$f_{\text{enamel}}$ [mGy (C kg) <sup>-1</sup> ]	Absorbed dose rate <sup>a</sup> (mGy s <sup>-1</sup> )
M60	1.51 mm Al	0.052	34	$3.82 \times 10^{-5}$	$2.27 \times 10^5$	8.66	—	—
M250	5.0 mm Al 3.2 mm Cu	3.2	138	$3.77 \times 10^{-5}$	$5.00 \times 10^4$	1.88	$5.88 \times 10^4$	2.20
<sup>137</sup> Cs	—	—	662	$4.05 \times 10^{-4}$	$3.51 \times 10^4$	1.42 <sup>b</sup>	$3.40 \times 10^4$	1.38 <sup>b</sup>
<sup>60</sup> Co	—	—	1250	$2.66 \times 10^{-4}$	$3.50 \times 10^4$	9.33 <sup>b</sup>	$3.38 \times 10^4$	9.02 <sup>b</sup>

<sup>a</sup>These columns are the products of the exposure rates and the factors for conversion of exposure to absorbed dose for human adult cortical bone and for tooth enamel.

<sup>b</sup>These were the dose rates at the beginning of the experiment; they were decay-corrected to the day of a particular experiment.

energy derived from half-value layer (HVL) measurements rather than spectrum averaging can lead to errors in estimated dose of as much as 24%. Finally, self-attenuation by thick samples could result in nonuniform irradiation, again most markedly at low energies.

We reviewed the work of Copeland *et al.* (2) and found that the composition of compact bone given in Report 10b of the International Commission on Radiation Units and Measurements (ICRU) (7), rather than the more current composition given in ICRU 44 (8), was used in the conversion of exposure to absorbed dose, and that an equivalent photon energy derived from HVL measurements was used in place of spectrum averaging. Based on our earlier work (6), these assumptions would lead to an underestimation of the dose delivered at low energies. Review of the work of Iwasaki *et al.* (5) showed that the energy dependence reported was for exposure, not absorbed dose. We thus hypothesized that the "apparent" energy dependence in EPR signal intensity reported in these previous studies was due to errors in estimating the delivered dose rather than to energy dependence.

Our long-term goal is to use EPR spectrometry of irradiated mineralized tissues in the dosimetry of bone-seeking radiopharmaceuticals which emit a wide range of photon energies (9) and in accidental overexposures (10, 11). The EPR dose-assessment method is based on additive reirradiation to generate a sample-specific calibration curve. In practice, bone samples with unknown doses are analyzed with an EPR spectrometer, and then additive known doses of radiation are delivered. The radiation-induced EPR signal intensity (ordinate) is measured at each dose (abscissa) increment, and the dose-response curve is back-extrapolated to the abscissa to obtain an estimate of the initial absorbed dose. Ideally, one would prefer to use  $\gamma$  radiation from a standard source (e.g. <sup>60</sup>Co) to assess the dose from a number of other radiation types. The energy dependence reported by previous investigators would limit the use of EPR dosimetry for this type of analysis.

In an attempt to clarify the previous reports of such an energy dependence, we have studied the radiation-induced

EPR signal derived from the crystalline matrix of human cortical bone from males and females ranging in age from 23 to 95 years, using the National Institute of Standards and Technology (NIST) X-ray beam codes M60 (34 keV) and M250 (138 keV), and <sup>137</sup>Cs (662 keV) and <sup>60</sup>Co (1250 keV)  $\gamma$  rays (12). We also studied bovine tooth enamel irradiated with the same beams, with the exception of M60.

## MATERIALS AND METHODS<sup>2</sup>

Fresh-frozen human bone samples from a tibia from a 23-year-old male and a femur from a 47-year-old male were obtained from the Georgia Tissue bank. Cadaver femur bones from a 72-year-old male and from 75- and 95-year-old females were obtained from the Stanford University Medical Center. All samples were cut with a diamond blade saw to a length of approximately 2 cm. The bones were air-dried in a biohazard hood for at least 48 h and then weighed. The average sample mass was about 70 mg, depending on the sample thickness (see below). Four bone segments were prepared for each subject at each energy, with the exception of samples from the 72-year-old male which were irradiated with <sup>60</sup>Co, where eight segments were used.

Upper anterior bovine jawbone sections were procured for the studies of tooth enamel. A dremmel tool was used to cut the teeth from the jaw at the gumline, and then the incisors were prepared in the following way. A high-speed lathe was used to sand down the sides of the tooth to facilitate mounting onto the diamond blade saw. The tooth was sliced parallel to the flat surface, which removed most of the dentin. The resulting slab was cut in the direction of the crystalline growth into samples approximately 2 cm wide. The high-speed lathe, and then a diamond-tipped dental drill, were used to complete the removal of the dentin. All samples were viewed under UV light to ensure that removal of dentin was complete, and then they were weighed.

The samples were irradiated using the NIST X-ray calibration facility (12) and the vertical  $\gamma$ -ray calibration beams. Table I provides specific information about the sources and their radiation output. Field size/uniformity and depth-dose measurements were made for each of the radiation fields with radiochromic films (13). For a field size of 5 × 5 cm, uniformity of about  $\pm 2$ –3% was obtained at all energies. Depth-dose pro-

<sup>2</sup>Mention of commercial products does not imply recommendation or endorsement by the NIST, nor does it imply that the products identified are necessarily the best for the purpose.

TABLE II  
Age and Sex of Each Human Subject and the Radiation Beams Studied  
[Indicated by Check (✓) Marks]

Subject no.	Age	Sex	Radiation beams			
			M60	M250	<sup>137</sup> Cs	<sup>60</sup> Co
1	47	male	✓	✓	✓	✓
2	23	male	✓	—	—	✓
3	75	female	✓	—	—	✓
4	72	male	—	—	—	✓
5	95	female	—	—	—	✓

files, acquired by placing radiochromic film in a wedge at a 9° angle, were used to determine the amount of build-up material needed for each beam. They were also used to derive dose estimates for bone segments irradiated with the M60 X-ray beam. B-110 (bone-equivalent plastic) holders were used for the  $\gamma$  irradiations (<sup>137</sup>Cs: 2 mm, <sup>60</sup>Co: 3 mm). X irradiations were conducted with the samples supported free-in-air on a block of styrofoam to remove radiation due to backscatter. Table II shows which samples were irradiated with each beam.

Dosimetry for each beam was conducted according to the methods described by Schauer *et al.* (6). In general, X-ray exposure rates were measured using the NIST 50- to 300-kV free-air chamber, and  $\gamma$ -ray exposure rates were measured with a 3-cm<sup>3</sup> air-equivalent ionization chamber. Conversion from exposure to absorbed dose was done using spectrum-averaged  $f$  factors, assuming the ICRU 44 (8) composition of cortical bone (6). In the case of <sup>137</sup>Cs, a monoenergetic  $f$  factor was used. For the tooth samples the dose was determined using the  $f$  factors calculated for tooth enamel ( $f_{\text{enamel}}$ ) given in Table I.

All samples were analyzed with a Bruker ESP300E spectrometer equipped with a transverse magnetic (TMH) resonator operating at approximately 9.85 GHz, with a modulation frequency of 100 kHz. The spectrometer settings for bone (and teeth) were microwave power 160 mW (200), modulation amplitude 0.2 mT (0.3) and gain  $1 \times 10^5$ . A time constant of 655 ms (328) was chosen based on a line width of 0.4 mT,

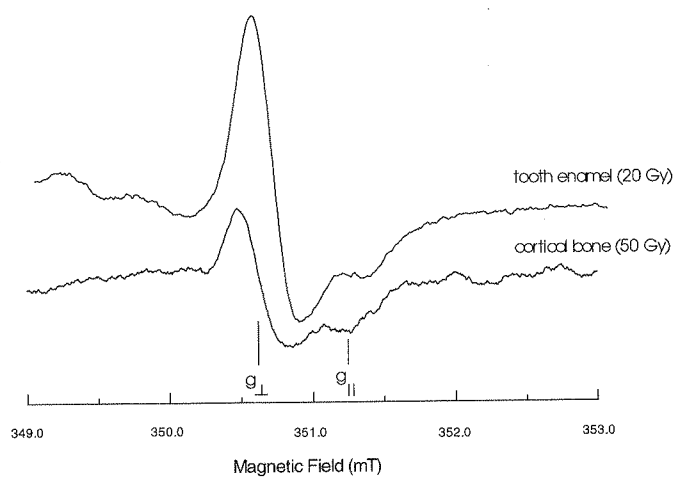


FIG. 1. First derivative of the absorption curve (arbitrary units) with respect to the applied magnetic field (mT) for a femur from a 47-year-old human male (50 Gy) and bovine tooth enamel (20 Gy) irradiated with <sup>60</sup>Co  $\gamma$  rays. The signal of interest in this study,  $g_{\perp}$  (2.0018), is derived from the crystalline matrix of bone or teeth.

a sweep width of 5 mT (10) and a sweep time of 84 s. The samples were marked to ensure reproducible positioning inside the quartz tubes. The EPR spectrum was constructed from the sum of 16 spectral scans for bone and 4 for enamel. All spectra were acquired as the first derivative of the absorption curve with respect to the applied magnetic field.

Sample-specific EPR calibration curves were generated using <sup>60</sup>Co  $\gamma$  rays as follows: bone segments were held in the 3-mm-thick, B-110 holders, and doses were added in 20-Gy increments over the range from 20 to 100 Gy. Least-squares linear regression (EPR signal intensity as a function of added dose) was then used to verify the initial doses.

To estimate the effects of sample self-attenuation of the incident beam, which could lead to an overestimation of the delivered dose, Monte Carlo calculations were performed. Since sample attenuation effects would be most pronounced at low photon energies, calculations of the dose in bone irradiated with the M60 X-ray beam were performed. When the secondary electrons have penetration ranges that are very small in comparison with the dimensions of interest and have radiative losses that are negligible, the absorbed dose from photon irradiation can be determined reliably from knowledge of the absorption and scattering of the photons in the target. This is the case for bone samples 0.5 to 2.0 mm thick irradiated by 60 kVp X-ray beams.

The dose was calculated on the basis of Monte Carlo calculations with the ETRAN code of Seltzer (14). One million photon histories, for perpendicular incidence with energies sampled from the spectral distribution of the NIST M60 X-ray calibration beam, were traced through plane slabs of bone thicknesses of 0.5, 1.0 and 2.0 mm until they either escaped or fell to an energy below 1 keV, at which point total absorption was assumed. The composition and density of the bone were taken from ICRU 44 (8). The absorbed dose was obtained for each bone thickness from scores of the amount of photon energy that escaped through all boundaries.

Plots of the radiation-induced EPR signal intensity ( $g_{\perp}$ ) as a function of photon energy report the normalized EPR signal intensity. All results are normalized for mass, dose (calculated or estimated) and the total number of EPR scans. The calculated dose is obtained from a conversion of exposure to absorbed dose, and the estimated dose is from the EPR (additive reirradiation) method. Tests of significant differences in EPR signal intensities were based on either a one-way analysis of variance (ANOVA) and Newman-Keuls multiple comparison tests or on Student's  $t$  tests. All critical values were based on an  $\alpha = 0.05$  level. There is only a 5% probability that we would reject the hypothesis of no difference in EPR signal intensities when no difference exists.

## RESULTS

Figure 1 shows typical spectra from cortical bone (50 Gy) and tooth (20 Gy) irradiated with <sup>60</sup>Co  $\gamma$  rays where the absorbed doses are expressed as dose in bone or tooth. Fig-

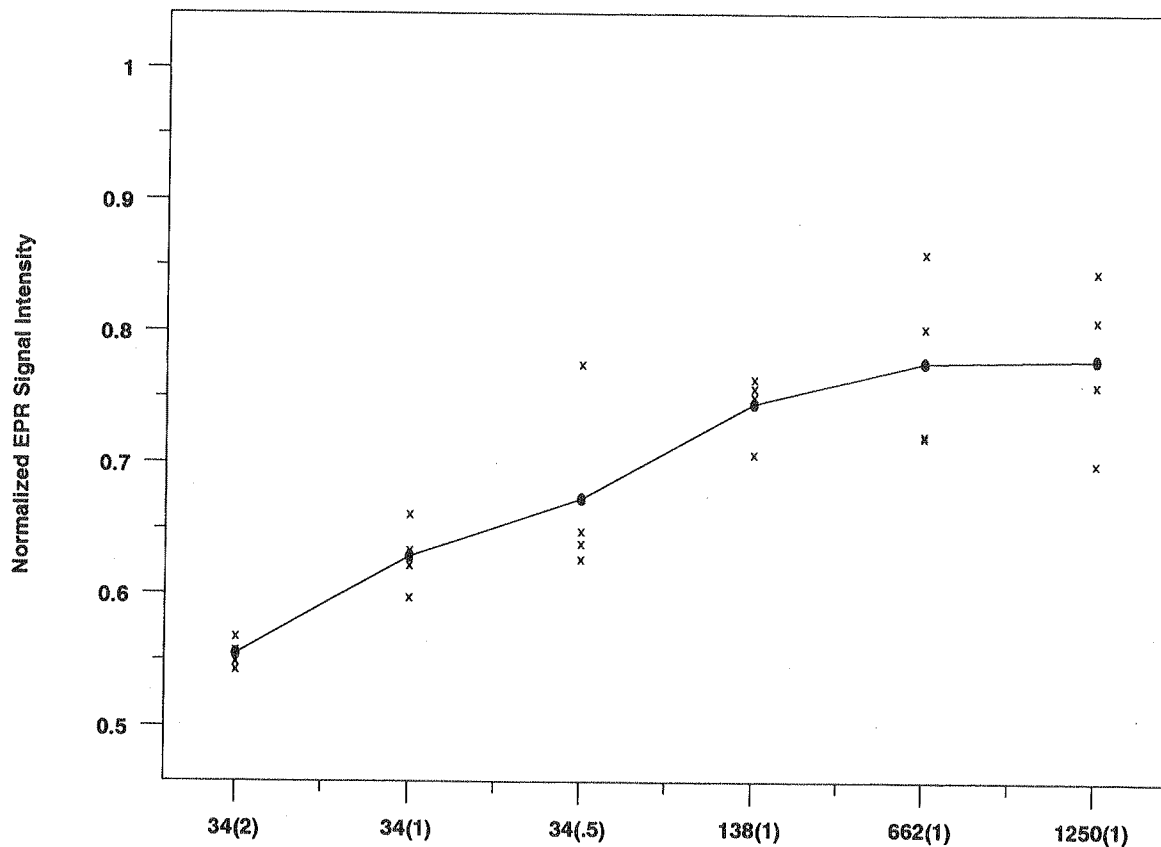


FIG. 2. Scatterplot of the raw ( $\times$ ) and mean ( $\bullet$ — $\bullet$ ) normalized EPR signal intensities vs photon energy for samples from subject 1 (47-year-old human male) ( $n = 4$  for each energy/thickness). Values are normalized for mass, an exposure to absorbed dose in bone of 50 Gy averaged over the mass of the bone, and total number of EPR scans. Bone thicknesses in mm are indicated in parentheses.

Figure 2 is a scatterplot of the raw and mean normalized EPR signal intensities ( $g_{\perp}$ ) from a femur from a 47-year-old human male (subject 1) as a function of photon energy. The data at 34 keV demonstrate a problem encountered with low-energy X-ray dosimetry. For the initial study, all samples were approximately 1 mm thick, and a dose in bone of 50 Gy, calculated using the conversion factors for exposure to absorbed dose in Schauer *et al.* (6), was delivered at each energy. The apparent reduced signal intensity at 34 keV for this thickness might be due to attenuation of the primary beam by the sample. The depth-dose profile for the M60 X-ray beam (Fig. 3) from the radiochromic film measurement revealed that the 1-mm sample was indeed receiving a nonuniform dose, possibly as much as 17% less in the back surface relative to the front surface. Thinner (0.5 mm) and thicker (2.0 mm) samples were then irradiated. Figure 2 shows a trend of increasing mean signal intensity with decreasing sample thickness. This is consistent with the fact that thinner bone samples receive a dose closer to the calculated 50 Gy, when averaged over the mass of the bone.

An estimate of the actual dose delivered was obtained by using the EPR (additive reirradiation) method. Sample-spe-

cific calibration curves were generated for one bone from each thickness from the M60-irradiated samples and one bone for each of the other energies. Figure 4 is the calibration curve for a 34 keV X-irradiated sample (0.5 mm). A summary of the measured depth-dose, Monte Carlo and EPR dose estimates is tabulated in Table III. There is relatively good agreement among these methods for the M60 X-ray beam. The most representative values are probably the EPR estimates since they are sample-specific and would show any differences in dose in a given material resulting from variation in assumed and actual elemental compositions.

In an attempt to account for any sample attenuation effects, we used the EPR estimates of delivered dose rather than the dose calculated from the conversion of exposure to absorbed dose to renormalize signal intensities. These results, given in Table IV, show a slight trend of progressively decreasing (4–15%) signal intensity with decreasing photon energy.

First, a test of the null hypothesis, or the hypothesis of no difference among EPR signal intensities induced by different energy photons, was performed. One-way ANOVA of the renormalized data yielded a test statistic of 2.68 ( $P = 0.055$ )

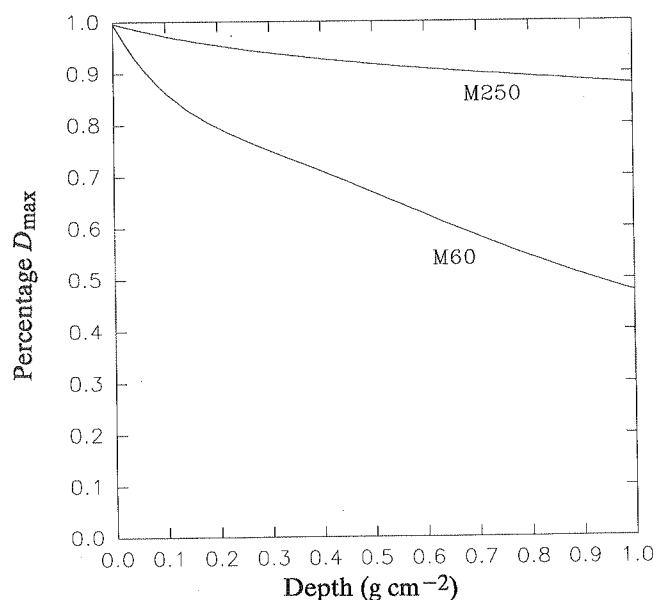


FIG. 3. Depth-dose profiles in B-110 (bone-equivalent plastic) for X-ray beams M60 (34 keV) and M250 (138 keV).

and the critical value was 2.77. Since the test statistic does not fall in the critical region, the null hypothesis is not rejected, and a conclusion of no statistically significant difference is reached. However, since the values are so close, further analysis of the data is needed.

Second, a Newman-Keuls multiple comparison test was performed. A comparison of the highest photon energy (1250 keV) and the lowest average photon energy results, yielded a test statistic that was close to the critical value, at the  $\alpha = 0.05$  level. Although this observation is suggestive of a statistical difference, it is marginal. Further comparisons revealed no statistically significant pairwise differences between the 1250 keV value and the remaining data (34 keV: 0.5 mm, 34 keV: 2 mm, 138 keV and 662 keV), and no difference between the 34 keV: 1-mm value and all other data (except the difference at 1250 keV described above).

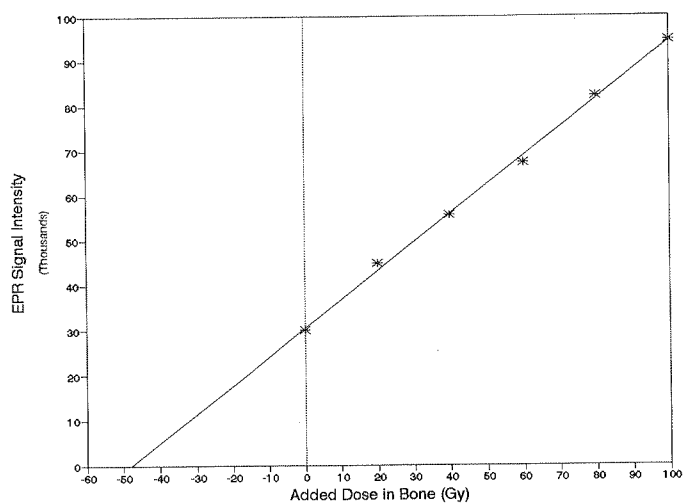


FIG. 4. EPR (additive reirradiation) calibration curve for a 0.5-mm bone sample irradiated with 34 keV average energy X rays. Added doses were delivered using  $^{60}\text{Co}$   $\gamma$  rays.  $r^2 = 0.9982$ .

The previous tests were intended to determine if a statistically significant difference exists in EPR signal intensity as a function of photon energy. A test was then performed to determine if a statistically significant trend of decreasing EPR signal intensity with decreasing photon energy exists. A least-squares linear regression fit of the mean EPR signal intensities (the 34 keV value was the mean for the three thicknesses) vs the square root of photon energy yielded a clear linear trend. In fact, a test of the null hypothesis of the slope of the line being equal to zero yielded a test statistic of 126.0 ( $P < 0.0001$ ). Therefore, the null hypothesis is rejected and the slope of the line is not equal to zero. The probability, by chance of four successive runs-up of length 1 or one run-up of length 4, is  $(1/2)^4$  or 6%. Therefore, either this is a rare event, or there is a statistically significant trend toward decreasing EPR signal intensity with decreasing photon energy.

Additional energy-dependence experiments were performed using 0.5-mm-thick human bone samples from a tibia

TABLE III  
Dose Estimates (Gy) from Depth-Dose Measurements in B-110, Monte Carlo Calculations Assuming the ICRU 44 Composition of Cortical Bone, and EPR (Additive Reirradiation) Analysis of Bone Samples from a Femur from a 47-Year-Old Male

Photon beam	Dose (Gy)		
	Depth-dose measurement	Monte Carlo calculation	EPR estimation (additive reirradiation)
M60 (2.0 mm)	40.7	38.1	39.3
M60 (1.0 mm)	43.8	43.6	46.4
M60 (0.5 mm)	46.0	47.0	48.0
M250	—	—	52.2
$^{137}\text{Cs}$	—	—	51.3
$^{60}\text{Co}$	—	—	49.4

TABLE IV  
Newman-Keuls Multiple Comparison Analysis of the Mean EPR Signal Intensities Normalized for Mass, EPR Dose Estimates and Total Number of EPR Scans

Energy (keV)	34 (1.0)	34 (0.5)	34 (2.0)	138 (1.0)	662 (1.0)	1250 (1.0)
Mean	0.672	0.700	0.706	0.712	0.756	0.788

Note. Femur from a 47-year-old human male. Energies are reported in keV, and bone thicknesses in mm are indicated in parentheses. No statistically significant difference at the  $\alpha = 0.05$  level was observed between the mean values which are underlined.

from a 23-year-old male and a femur from a 75-year-old female. Eight samples that were prepared for each subject were divided into groups of four. Each group was irradiated with either the M60 X-ray beam or with  $^{60}\text{Co}$   $\gamma$  rays. Figure 5 is a plot of the raw and mean EPR signal intensities normalized for mass, EPR dose estimates and total number of EPR scans. The EPR dose estimates (Gy) for the sample from the 23-year-old male were M60, 47.9, and  $^{60}\text{Co}$ , 48.8,

and for the sample from the 75-year-old female, M60, 45.1 and  $^{60}\text{Co}$ , 48.1. Figure 5 shows that there is a 4% higher mean signal intensity at M60 compared to  $^{60}\text{Co}$  for the 23-year-old and a 12% lower mean signal intensity at M60 compared to  $^{60}\text{Co}$  for the 75-year-old. A  $t$  test of the difference between two means for each set of data shows no statistically significant difference between the M60 and  $^{60}\text{Co}$  values for each subject. The computed  $P$  values for these com-

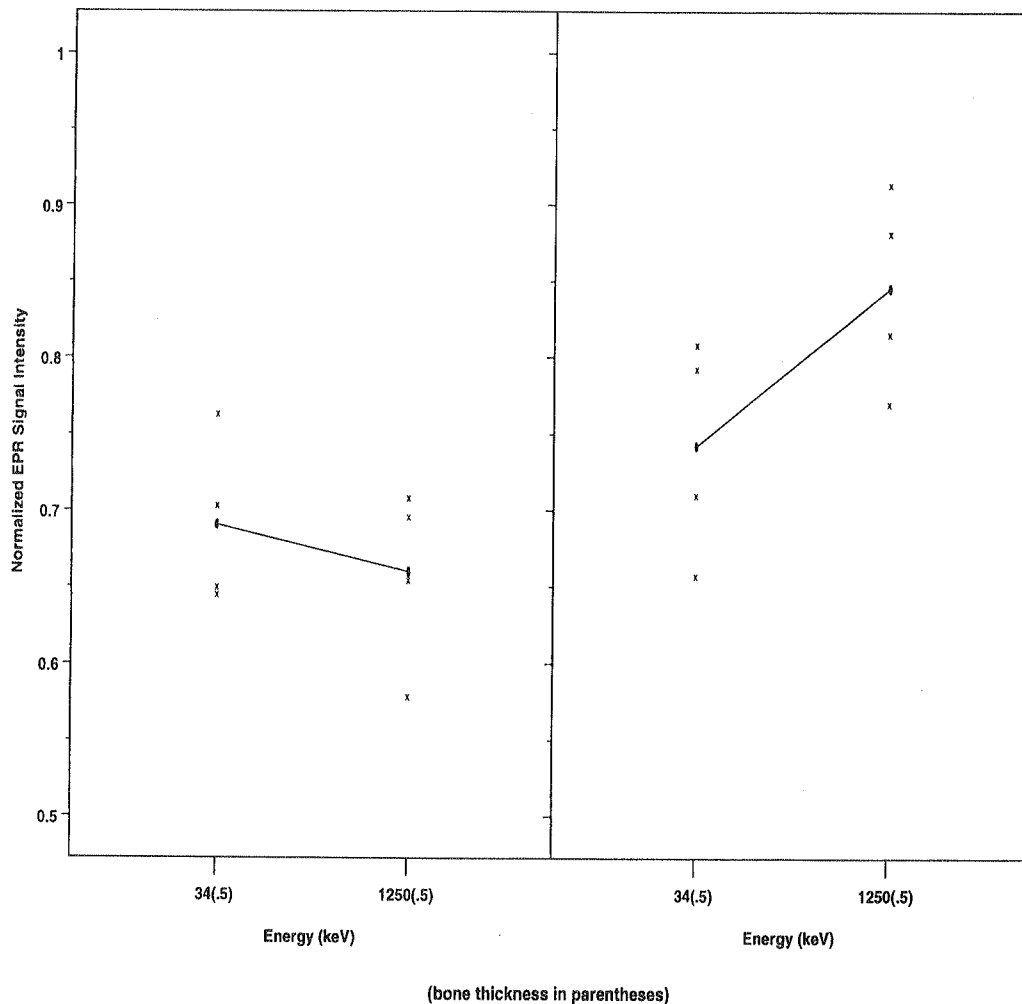


FIG. 5. Scatterplot of the raw ( $\times$ ) and mean ( $\bullet$ — $\bullet$ ) normalized EPR signal intensity vs photon energy for (left panel) samples from subject 2 (23-year-old human male) and (right panel) subject 3 (75-year-old human female) ( $n = 4$  for each subject at each energy). Values are normalized for mass, EPR dose estimate and total number of EPR scans. Bone thicknesses in mm are indicated in parentheses.

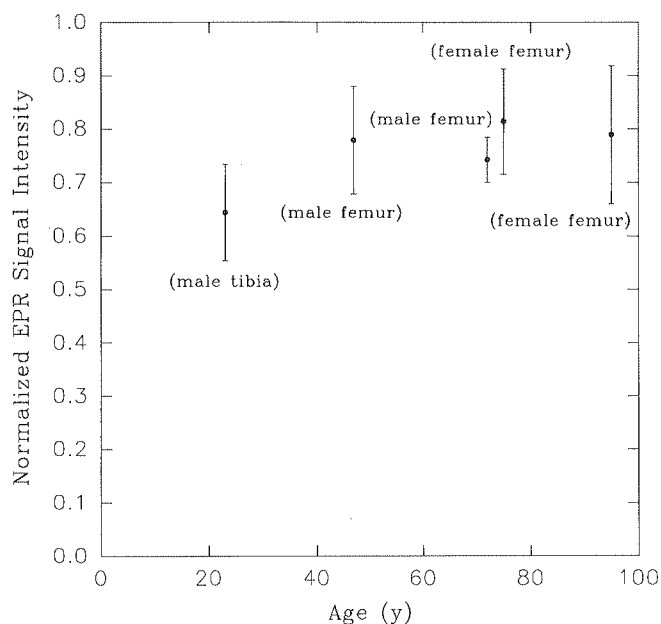


FIG. 6. Mean normalized EPR signal intensity and 95% confidence interval for the  $^{60}\text{Co}$ -irradiated samples from 23-, 47- and 72-year-old males and 75- and 95-year-old females. Values are normalized for mass, calculated dose (50 Gy) and total number of EPR scans.

parisons were  $P = 0.49$  for the data for the 23-year-old male, and  $P = 0.076$  for the data for the 75-year-old female.

To study possible differences in signal intensities between human males and females of different ages, the EPR signal intensities for the  $^{60}\text{Co}$ -irradiated samples from 23-, 47- and 72-year-old males and 75- and 95-year-old females were compared. Average signal intensities normalized for mass, calculated dose (50 Gy) and number of EPR scans are plotted in Fig. 6. Four samples were analyzed for each subject, except that for the 72-year-old male, which included eight bones. This energy ( $^{60}\text{Co}$ ) was chosen because significantly large differences in elemental composition, like those noted between ICRU 10b and ICRU 44, will not change the dose appreciably (6). Indeed, there is good agreement between the calculated dose (50 Gy) and the EPR estimated doses (e.g., 23-year-old = 48.8 Gy, 47-year-old = 49.4 Gy, and 75-year-old = 48.1 Gy). Figure 6 shows a 21% lower mean signal intensity for the tibia from the 23-year-old male, compared to the rest of the values.

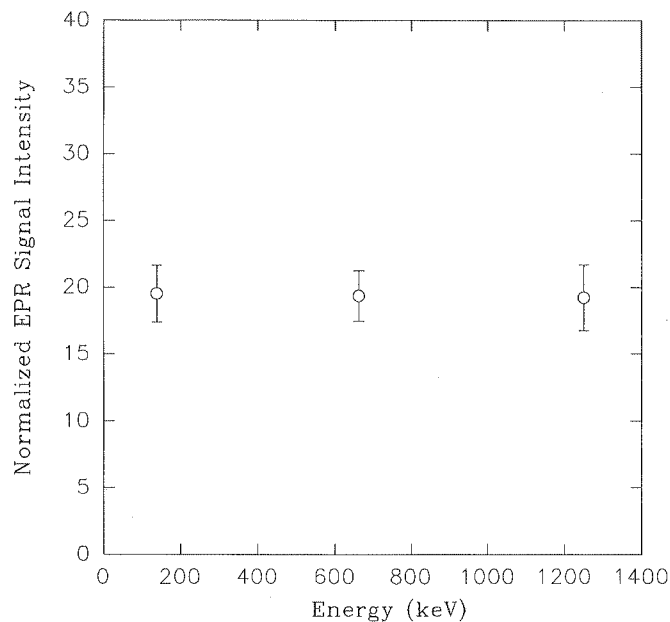


FIG. 7. Mean normalized EPR signal intensity and 95% confidence interval for bovine tooth enamel vs photon energy. All values are normalized for mass, calculated dose (50 Gy) and total number of EPR scans.

One-way ANOVA of these data yielded a test statistic of 5.26 ( $P = 0.015$ ) and the critical value was 3.49. Since the test statistic falls in the critical region, the null hypothesis is rejected. The Newman-Keuls multiple comparisons test was used to identify where the differences exist. Analysis of the samples from the 23- and 47-year-old males and the 75- and 95-year-old females revealed a statistically significant difference at the  $\alpha = 0.05$  level between the young male subject and all others, but no differences were found among the others (Table V).

The results for bovine tooth enamel are shown in Fig. 7. The radiation-induced EPR signal intensities are essentially the same, within a 95% confidence interval. As expected, the data for enamel are consistent with the results for bone. These results are in agreement with the observation of no significant difference between EPR signal intensities for tooth enamel irradiated to the same absorbed dose with low-energy X rays and  $^{60}\text{Co}$   $\gamma$  rays (3).

TABLE V  
Newman-Keuls Multiple Comparison Analysis of the Mean EPR Signal Intensity of  $^{60}\text{Co}$ -Irradiated Bone Samples Normalized for Mass, Calculated Dose and Total Number of EPR Scans

Age (years)	23, male	47, male	95, female	75, female
Mean	0.644	0.779	0.789	0.814

Note. No statistically significant difference at the  $\alpha = 0.05$  level was observed between the mean values which are underlined.

## DISCUSSION

We have demonstrated experimentally that the radiation-induced EPR signal intensity derived from the crystalline matrix of human cortical bone does not increase with decreasing photon energy. Instead, in samples from two of three subjects (23-year-old male and 75-year-old female) no statistically significant differences at the  $\alpha = 0.05$  level in EPR signal intensity as a function of photon energy were observed, and in samples from the third subject the only difference was between one of the 34 keV data sets and the  $^{60}\text{Co}$  values.

In samples from two of three subjects (47-year-old male and 75-year-old female), however, a progressive trend toward decreasing (12–15%) EPR signal intensity with decreasing photon energy was observed even after correction for sample attenuation effects. Analysis of these data for the samples from the 47-year-old male revealed that the slope of a least-squares linear regression fit of the mean EPR signal intensity data vs the square root of photon energy was not equal to zero. This trend, which might be more pronounced at lower photon energies than those studied here, could be due to a dependence of the EPR response on the density of ionization along the secondary electron tracks. Such a linear energy transfer (LET) effect, as it relates to thermoluminescent dosimeters, has been reported previously by Attix (15). In general, recombination of ions could result in decreased energy use. Aldrich and Pass (16) observed a similar trend in dental enamel.

There is insufficient information to recommend the use of energy-dependent correction factors at low photon energies. However, investigators should be aware that the radiation-induced EPR signal derived from the crystalline matrix of bone and teeth does not increase with decreasing photon energy. In fact, decreases of up to 15% may be seen.

A comparison of the mean EPR signal intensities of bone irradiated with  $^{60}\text{Co}$   $\gamma$  rays for the 23- and 47-year-old males and the 75- and 95-year-old females revealed a statistically significant difference at  $\alpha = 0.05$  between the data for the youngest subject and all others. This is probably not due to variation in elemental composition, since even large differences do not alter the conversion of exposure to absorbed dose. It could be at least partly due to differences in crystallinity.

Our study demonstrates the importance of several factors in the dosimetry of mineralized tissues. The most significant factors are the choice of elemental composition for bone and enamel, the use of spectrum averaging rather than using equivalent photon energies derived from HVL measurements, and self-attenuation effects. Previous studies of energy dependence neglected to consider one or more of these factors which led to conflicting results.

The most important application of bone and tooth EPR dosimetry is retrospective dose assessment. In particular, reliable dose estimates are essential to the quality of long-term epidemiological studies, for example, those under way for individuals exposed in the Chernobyl accident. Ultimately, EPR dose estimates for this group may be used to assess the health effects of low-level ionizing radiation. Therefore, we recommend that these dosimetry factors be considered in future studies.

## ACKNOWLEDGMENTS

The authors wish to thank Susan Knox, M.D., and Carol Marquez, M.D., from the Stanford University Medical Center for providing the cadaver bone samples, Paul Lamperti and Debra Benson for their assistance with the radiation sources, James Filliben and Stefan Leigh for their help with the statistical analysis of the data, and Edward Parry (American Dental Association) for the use of dental equipment and his advice for enamel preparation. This work was supported by the U.S. Navy Health Sciences Education and Training Command, the Department of Energy and the Defense Nuclear Agency. The views expressed in this article are those of the authors and do not reflect the official policy or position of the U.S. Navy or the Department of Defense.

Received: July 8, 1993; accepted: October 22, 1993

## REFERENCES

1. W. Stachowicz, J. Michalik, A. Dziedzic-Goclawska and K. Ostrowski, Evaluation of absorbed dose of gamma and x-ray radiation using bone tissue as a dosimeter. *Nukleonika* **19**, 845–850 (1974).
2. J. F. Copeland, K. R. Kase, G. E. Chabot, F. T. Greenaway and G. B. Inglis, Spectral energy effects in ESR bone dosimetry: photons and electrons. *Appl. Radiat. Isot.* **44**, 101–106 (1993).
3. B. Pass and J. E. Aldrich, Dental enamel as an *in vivo* radiation dosimeter. *Med. Phys.* **12**, 305–307 (1985).
4. V. A. Serezhnev, E. V. Domracheva, G. A. Klevezal, S. M. Kulikov, S. A. Kuznetsov, P. I. Mordvintsev, L. I. Sukhovskaya, N. E. Schklovsky-Kordi, A. F. Vanin, V. V. Voevodskaya and A. I. Vorobiev, Radiation dosimetry for residents of the Chernobyl region: A comparison of cytogenetic and electron spin resonance methods. *Radiat. Prot. Dosim.* **42**, 33–36 (1992).
5. M. Iwasaki, C. Miyazawa, A. Kubota, E. Suzuki, K. Sato, J. Naio, A. Katoh and K. Niwa, Energy dependence of the  $\text{CO}_3^{2-}$  signal intensity in ESR dosimetry of human tooth enamel. *Radioisotopes* **40**, 421–424 (1991).
6. D. A. Schauer, S. M. Seltzer and J. M. Links, Exposure-to-absorbed-dose conversion for human adult cortical bone. *Appl. Radiat. Isot.* **44**, 485–489 (1993).
7. ICRU, *Physical Aspects of Irradiation*. Report 10b, NBS Handbook 85, International Commission on Radiation Units and Measurements, Bethesda, MD, 1964.
8. ICRU, *Tissue Substitutes in Radiation Dosimetry and Measurement*. Report 44, International Commission on Radiation Units and Measurements, Bethesda, MD, 1989.
9. M. F. Desrosiers, M. J. Avila, D. A. Schauer, B. M. Coursey and N. J. Parks, Experimental validation of radiopharmaceutical absorbed dose to mineralized bone tissue. *Appl. Radiat. Isot.* **44**, 459–463 (1993).
10. M. F. Desrosiers, *In vivo* assessment of radiation exposure. *Health Phys.* **61**, 859–861 (1991).
11. D. A. Schauer, B. M. Coursey, C. E. Dick, W. L. McLaughlin, J. M. Puhl, M. F. Desrosiers and A. D. Jacobson, A radiation accident at an industrial accelerator facility. *Health Phys.* **65**, 131–140 (1993).
12. P. J. Lamperti, T. P. Loftus and R. Loevinger, *Calibration of X-ray and Gamma-ray Measuring Instruments*. Special Publication 250-16, National Institute of Standards and Technology, Gaithersburg, MD, 1988.
13. W. L. McLaughlin, C. Yun-Dong, C. G. Soares, A. Miller, G. Van Dyk and D. F. Lewis, Sensitometry of the response of a new radiochromic film dosimeter to gamma radiation and electron beams. *Nucl. Instrum. Meth. Phys. Res.* **A302**, 165–176 (1991).
14. S. M. Seltzer, Electron-photon Monte Carlo calculations: The ETRAN code. *Appl. Radiat. Isot.* **42**, 917–941 (1991).
15. F. H. Attix, Basic gamma-ray dosimetry. *Health Phys.* **15**, 49–94 (1968).
16. J. E. Aldrich and B. Pass, Dental enamel as an *in vivo* radiation dosimeter: Separation of the diagnostic dose from the dose due to natural sources. *Radiat. Prot. Dosim.* **17**, 175–179 (1986).